ELSEVIER

Journal of Environmental Management 85 (2007) 649–658

Journal of Environmental Management

www.elsevier.com/locate/jenvman

Application of a new leaf area index algorithm to China's landmass using MODIS data for carbon cycle research

R. Liu[a,*], J.M. Chen[b], J. Liu[a], F. Deng[b], R. Sun[c,d,e]

[a]*State Key Laboratory of Resources and Environmental Information System, Institute of Geographical Sciences and Natural Resources Research, Chinese Academy of Sciences, No.11A, Datun Road, Chaoyang, Beijing, 100101, China*

[b]*Department of Geography and Program in Planning, University of Toronto, 100 St. George St., Room 5047,Toronto, Ont., Canada M5S 3G3*

[c]*School of Geography, Beijing Normal University, Beijing, China*

[d]*State Key Laboratory of Remote Sensing Science, Beijing, China*

[e]*Beijing Key Laboratory for Remote Sensing of Environment and Digital Cities, Beijing, China*

Received 6 January 2006; received in revised form 3 March 2006; accepted 4 April 2006
Available online 22 November 2006

Abstract

An operational system was developed for mapping the leaf area index (LAI) for carbon cycle models from the moderate resolution imaging spectroradiometer (MODIS) data. The LAI retrieval algorithm is based on Deng et al. [2006. Algorithm for global leaf area index retrieval using satellite imagery. IEEE Transactions on Geoscience and Remote Sensing, 44, 2219–2229], which uses the 4-scale radiative transfer model [Chen, J.M., Leblancs, 1997. A 4-scale bidirectional reflection model based on canopy architecture. IEEE Transactions on Geoscience and Remote Sensing, 35, 1316–1337] to simulate the relationship of LAI with vegetated surface reflectance measured from space for various spectral bands and solar and view angles. This algorithm has been integrated to the MODISoft® platform, a software system designed for processing MODIS data, to generate 250 m, 500 m and 1 km resolution LAI products covering all of China from MODIS MOD02 or MOD09 products. The multi-temporal interpolation method was implemented to remove the residual cloud and other noise in the final LAI product so that it can be directly used in carbon models without further processing. The retrieval uncertainties from land cover data were evaluated using five different data sets available in China. The results showed that mean LAI discrepancies can reach 27%. The current product was also compared with the NASA MODIS MOD15 LAI product to determine the agreement and disagreement of two different product series. LAI values in the MODIS product were found to be 21% larger than those in the new product. These LAI products were compared against ground TRAC measurements in forests in Qilian Mountain and Changbaishan. On average, the new LAI product agrees with the field measurement in Changbaishan within 2%, but the MODIS product is positively biased by about 20%. In Qilian Mountain, where forests are sparse, the new product is lower than field measurements by about 38%, while the MODIS product is larger by about 65%.

Keywords: Leaf area index; MODIS 4-scale model; China

1. Introduction

The leaf area index (LAI), defined as one-half the total green leaf area per unit ground area for both needleleaf and broadleaf canopies (Chen and Black, 1992), is a key parameter controlling many biological and physical processes associated with vegetation on the earth's surface, such as photosynthesis, carbon and nutrient cycle, radiative balance, evapotranspiration, and rainfall interception. Thus, LAI is widely used to drive models of ecology, hydrology, biogeochemistry and climate (Sellers et al., 1996). For effective use in large-scale models, this parameter should be collected over a long period of time and cover large regions with different land surface types. Remote sensing technology is the only available means to achieve this goal. Since the LAI value affects remote sensing signals at different wavelengths, regional and global LAI maps can be derived from multi-spectral remote sensing imagery.

*Corresponding author. Tel.: +86 10 64889466; fax: +86 10 64855049.
E-mail addresses: liurg@lreis.ac.cn, lronggao@yahoo.com (R. Liu).

0301-4797/$ - see front matter © 2006 Elsevier Ltd. All rights reserved.
doi:10.1016/j.jenvman.2006.04.023

Estimating LAI from optical remote sensing data can generally be carried out by two different approaches. One is based on empirical relationships between field measurements of LAI and vegetation indices (VI) from satellite data, and another utilizes physically based canopy reflectance models by applying model inversion techniques (Liang, 2003). The VI-based models have various mathematical forms for different land cover types in different regions (Turner et al., 1999; Chen et al., 2002). It is problematic to apply this approach to a large area because the LAI-VI relationship would vary spatially and temporally under various conditions of observation from space, even for the same surface cover type. The inversion of a radiative transfer model is the only possible way to retrieve LAI maps for large regions (Chen et al., 2002), but direct model inversions to estimate LAI are often time consuming and not practical for regional and global image processing. Usually, efficient pixel-based inversions of radiative models are made using various techniques, such as optimization (Liang, 2003), look-up tables (Myneni et al., 2002), and the neural networks (Fang et al., 2003).

The launches of MODIS twin sensors on December 18, 1999 aboard the Terra satellite and on May 04, 2002 aboard the Aqua satellite, began a new era in remote sensing of the Earth's surface. The 36 spectral bands and highest spatial resolution at 250 m for visible and near infrared bands enhance MODIS ability for a systematic monitoring of land, atmosphere and oceans. These characteristics of high spectral resolution, high temporal resolution and medium spatial resolution make MODIS a powerful sensor for LAI mapping (Myneni et al., 2002). A global LAI product (MOD15) is being routinely generated with 1-km resolution at 8-day intervals and can be downloaded from the National Aeronautics and Space Administration (NASA) data center (Myneni et al., 2002). It is derived from the red (648 nm) and near-infrared (858 nm) bands of the surface reflectance product (MOD09), using land cover type product (MOD12) and ancillary information on surface characteristics as background (Wang et al., 2001). The retrievals are performed by comparing observed and modeled surface reflectances for a suite of canopy structures and soil patterns that covers a range of expected natural conditions. A three-dimensional radiative transfer model is used to derive spectral and angular biome-specific optical signatures. Should this main algorithm fail, a back-up algorithm is triggered to estimate LAI using a LAI-NDVI relationship (Knyazikhin et al., 1999). The MODIS LAI products have evolved through four versions so far. The latest version is the Collection 4, which has improved input data (surface reflectance data and biome map) and algorithm physics (LUTs and compositing) compared with Collection 3.

For regional applications, a global product may not be most suitable, and there is still much room for improvement. In particular, the MODIS LAI product was reported to be positively biased when compared with field measurements in many regions (Cohen et al., 2003). These limitations provide reasons for exploring various alternative approaches.

Deng et al. (2006) developed a new global LAI mapping algorithm to meet the requirement of the GLOBCARBON project (Plummer et al., 2004) for generating LAI products from different sensors. Their algorithm utilizes a geometrical optical and radiative transfer model to simulate the relationship between LAI and land surface reflectance in various illumination and observation angles under various canopy structural conditions, thus permitting the integration of the bidirectional reflectance distribution function (BRDF) into the LAI retrieval algorithm. This method differs from their previous method (Chen et al., 2002) which requires BRDF normalization to the input images. This new algorithm has the potential to use the angular variation as a source of information in LAI retrieval. A new software system MODISoft® was specifically developed for processing MODIS data in the Institute of Geographical Sciences and Natural Resources Research, Chinese Academy of Sciences. This system can process MODIS 1B data operationally and generate various products.

In this paper, a system which integrated Deng et al. (2006)'s LAI algorithm into MODISoft® to generate the LAI coverages using MODIS data in support of China carbon cycle research is presented. This includes a description of the salient features of the Deng et al. (2006)'s algorithm, evaluation of its performance and initial results of validation with field data. A multitemporal smoothing and interpolation method of Lv et al. (2006) was implemented to remove the residual cloud and other noise from the LAI product so it can be used to drive carbon cycle models.

2. Methods and data

2.1. Theoretical basis for LAI algorithms

A detailed description of the BRDF-based LAI retrieval technique was given by Deng et al. (2006). Here we simply describe its basic theory and procedures.

The relationship between the effective LAI (L_E) and the true LAI is defined as (Chen and Leblanc, 1997)

$$\mathrm{LAI} = L_E/\Omega, \tag{1}$$

where Ω is the clumping index.

LAI can be retrieved from red and near infrared (NIR) bands only or from shortwave infrared (SWIR), red and NIR bands. Using SWIR information has the advantages that (i) the algorithm is not sensitive to the vegetation background variation and (ii) the error in LAI due to error in input land cover information is reduced. These two separate algorithms are used to estimate the effective LAI independently:

$$L_E = f_{LE\_SR}(SR \cdot f_{BRDF}(\theta_v, \theta_s, \phi)); \tag{2}$$

$$L_E = f_{LE\_RSR}\left(SR \cdot f_{BRDF}(\theta_v, \theta_s, \phi) \times \left(1 - \frac{\rho_{SWIR} \cdot f_{SWIR\_BRDF}(\theta_v, \theta_s, \phi) - \rho_{SWIR\ min}}{\rho_{SWIR\ max} - \rho_{SWIR\ min}}\right)\right), \quad (3)$$

where SR is the ratio of NIR reflectance over red reflectance; ρ_{SWIR} is the band 5 reflectance for MODIS; $\rho_{SWIR\,max}$ is the maximum value of SWIR and $\rho_{SWIR\,min}$ is the minimum value of SWIR, both being determined from 1% cutoff points in the histogram of the input SWIR image; f_{LE_RSR} and f_{LE_RSR} are functions defining the relationships between L_E and SR and between L_E and the reduced simple ratio (RSR) (Brown et al., 2000) at a specific view and sun angle combination (θ_v,θ_s,ϕ_s). Functions f_{BRDF} and f_{SWIR_brdf}, quantifying the BRDF effects, depend on the angular reflectance behavior of the spectral bands involved, which are described mathematically based on a modified Roujean's model (Chen and Leblanc, 1997; Roujean et al., 1992):

$$\rho(\theta_v, \theta_s, \phi) = \rho_0(0,0,\phi)\left(1 + a_1 f_1(\theta_v, \theta_s, \phi) + a_2 f_2(\theta_v, \theta_s, \phi)\right)\left(1 + c_1 e^{-\left(\xi / \pi\right) c_2}\right), \quad (4)$$

where the last term involving c_1 and c_2 is the modification made by Chen and Cihlar (1997) to consider pronounced hotspot effects and has importance when the view angle is close to the sun angle, although it introduces two additional parameters and makes the equation non-linear. Functions f_1 and f_2 in Eq. (4) are defined as

$$f_1(\theta_v, \theta_s, \phi) = \frac{1}{2\pi}[(\pi - \phi)\cos\phi + \sin\phi] \times \tan\theta_s \tan\theta_v - \frac{1}{\pi}\left(\tan\theta_s + \tan\theta_v + \sqrt{\tan^2\theta_s + \tan^2\theta_v - 2\tan\theta_s\tan\theta_v\cos\phi}\right), \quad (5)$$

$$f_2(\theta_v, \theta_s, \phi) = \frac{4}{3\pi}\frac{1}{\cos\theta_s + \cos\theta_v} \times \left[\left(\frac{\pi}{2} - \xi\right)\cos\xi + \sin\xi\right] - \frac{1}{3}. \quad (6)$$

$\rho(\theta_v, \theta_s, \phi)$ can be obtained from atmospherically corrected remotely sensed land surface reflectance; and given values of a_1, a_2, c_1 and $c_2, \rho_0(0,0,\phi)$ can be calculated from the above formulas. From $\rho_0(0,0,\phi)$, $\rho(\theta_v, \theta_s, \phi)$ can be estimated at any angle combination. The BRDF kernel coefficients a_1, a_2, c_1, and c_2 are all based on the modelling results of the 4-scale geometrical optical model (Chen and Leblanc, 1997) for different land cover types.

The challenge in integrating BDRF into LAI algorithms is that the equations describing BRDF are non-linear and the coefficients a_1, a_2 depend on L_E. Thus, several iterations are required in the retrieval procedure to get the best fit between a_1, a_2 and L_E. To speed up the convergence, a Chebyshev polynomials-based technique was developed: (1) a precursor effective LAI value for a pixel is first estimated from a general cover-type dependent SR-LAI relationship, (2) BRDF kernels are calculated using the precursor effective LAI value, (3) final effective LAI is calculated from the BRDF kernels and SR/RSR, and (4) empirical clumping index for the land cover type is used to calculate the final LAI.

The 4-scale model for LAI simulation is complex and time-consuming. A look-up table technique was therefore developed to mimic various relationships developed through 4-scale. The solar zenith angle (SZA) is divided into 6 ranges: [0, 10], (10, 20], (20, 30], (30, 40], (40, 50], (50, 80]. For each SZA range, a set of relationships between L_E and SR (f_{LE_SR}) is provided at different view zenith angles (VZA) at two relative azimuth angles (ϕ) 0° and 180°. A linear interpolation is used to obtain the relation at different ϕ values for the first approximation of L_E. For each SZA range, $a_1(L_E)$ and $a_2(L_E)$ functions are provided to calculate the relevant parameters. The parameters c_1 and c_2 are given in advance, so the SR and ρ_{SWIR} can be estimated at any angle combinations. L_E is then calculated using the relationships between L_E and SR (f_{LE_SR}) and between L_E and RSR (f_{LE_SR}) at specific angles. The LAI can be calculated from L_E by formula (1) using empirical clumping index (Ω) values for different land cover types (Table 1).

2.2. The MODISoft® software for MODIS data processing

MODIS provides the most comprehensive remote sensing measurements from space so far, but few available commercial remote sensing software programs can process these data correctly to extract earth surface parameters. In order to effectively utilize these data, NASA designed 44 standard products and established four scientist teams covering land, atmosphere, ocean and calibration to develop the retrieval algorithms. Several standard products can be downloaded from the NASA data center. Although, NASA undertook many efforts to establish the global satellite product algorithm, its MODIS standard products are not well suited for Chinese land cover conditions. In addition, additional terrestrial parameters (to the designed 44 standard parameters) are needed to retrieve information from MODIS data. These requirements motivated us to develop the MODISoft® software for an automated processing of the large-volume, multi-temporal MODIS data so that standard products could be generated for terrestrial applications over China (Liu et al., 2006). The MODISoft® was developed in C code in July 2002, and the first version was published in December 2002 with four modules: basic, atmosphere, land and monitoring. It can produce standard products from MODIS 1B data, grid and composite them to remove the cloud and noise effects. A friendly graphic user interface (GUI) was designed to assist the operator in data input, display, product generation and output. A powerful console command was also provided to

Table 1
Grouping of IGBP land cover types into six functional types used in the new LAI algorithms and their clumping index

IGBP class	Class name	Coefficients group	Clumping index
1	Evergreen needleleaf forest	Conifer	0.6
2	Evergreen broadleaf forest	Tropical	0.8
3	Deciduous needleleaf forest	Conifer	0.6
4	Deciduous broadleaf forest	Deciduous	0.8
5	Mixed forest	Mixed forest	0.7
6	Closed shrublands	Shrub	0.5
7	Open shrublands	Shrub	0.5
8	Woody savannas	Shrub	0.5
9	Savannas	Shrub	0.9
10	Grasslands	Crop, grass, and others	0.9
11	Permanent wetlands	Crop, grass, and others	0.9
12	Croplands	Crop, grass, and others	0.9
13	Urban and built-up	Crop, grass, and others	0.9
14	Cropland mosaics	Crop, grass, and others	0.9
15	Snow/Ice		
16	Barren or sparsely vegetated		
17	Water bodies		

permit users to process data in batch mode, which is especially useful for processing voluminous data sets that need long run-times.

Several terrestrial parameters in MODIS products have been defined and produced by NASA, including: land surface reflectance (MOD09), land surface temperature (LST, MOD11), land cover classification (LCC, MOD12), vegetation indices (VI, MOD13), thermal anomalies (MOD14) and burned scar (MOD40), leaf area index (LAI, MOD15), MODIS Surface Resistance and Evapotranspiration (ET, MOD16), Vegetation Production and Net Primary Production (NPP, MOD17), Surface Reflectance BRDF/Albedo Parameter (MOD43), Vegetation Cover Conversion and Vegetation Continuous Fields (MOD44). Except for MOD16, these standard products can be downloaded from the NASA web site. However, to avoid large bias existing in some products and thus produce higher-quality regional products, MODISoft® has implemented several new algorithms and integrated Chinese local environmental background data. So far, several products (land surface reflectance (MOD09), land cover classification (MOD12), land burned scar (MOD12 and MOD40) and photosynthetically active radiation) have been produced from MODIS level 1B data (MOD02) using the new designed algorithm and local background data as input.

For the LAI product, Deng et al.'s algorithm (2006) was integrated to MODISoft®. This module uses MODIS MOD02 or MOD09 product as input and also provides several quality flags, including clear sky, cloud, uncertain, and snow/ice. The input data employs HDF format and the output data is in geotiff or HDF formats.

2.3. Input data for implementing the LAI algorithm

2.3.1. Land cover map

The LAI retrieval algorithm is land cover type-dependent. Land cover is stratified into six canopy architectural types or biomes (grasses and cereal crops, conifer, tropical, deciduous, mixed forest, shrub) and one non-vegetation class. These biomes represent the structural variations along the horizontal and vertical dimensions, canopy height, leaf type of herbaceous and woody vegetation. The land cover map reduces the number of unknowns in the LAI retrieval through simplifying assumptions (e.g., model leaf normal orientation distributions) and fixed constants (e.g., leaf, wood, litter and soil optical properties) that are assumed to vary with biome and soil types only (Myneni, et al., 2002). Except for the non-vegetation class, the same biome is set the same coefficients for LAI retrieval. The biomes classes can be derived from the IGBP land cover classes. The 14 IGBP vegetation types regrouped into the six functional types are shown in Table 1.

Several land cover data sets are available for all of China, such as the GLC 2000 and the MODIS MOD12 product. In this study, a regional land cover classification data set NLCD LCC from the year 2000 was used because it has been validated extensively in China (Liu et al., 2003). NLCD LCC was produced from the classification of one year of AVHRR composite data and other geophysical data sets. Prior to classification, China was divided into nine climatic regions using the mean climatic conditions over 10 years. For each region, the training data were selected from Landsat Thematic Mapper (TM) and survey maps. The 1-year 10-day composite AVHRR band 1, band 2 and the derived NDVI, plus mean annual temperature, mean annual precipitation, and elevation were classified by a supervised classification algorithm to generate land cover maps for individual regions. The nine land-cover maps were then assembled into one contiguous coverage (Liu et al., 2003). The NLCD LCC data set consisted of eighteen land cover classes: evergreen needleleaf forest, deciduous needleleaf forest, evergreen broadleaf forest, deciduous broadleaf forest, mixed forest, alpine forest, shrub, dense

grassland, moderate dense grassland, sparse grassland, cropland, wetland, city, water body, ice and snow, harsh desert, sandy desert, and bare rock. To correspond with the biomass type for LAI retrieval, the NLCD LCC data set is regrouped to six functional biomes according to Table 1.

2.3.2. MODIS data

The remote sensing data used to drive the LAI algorithm include land surface reflectance of MODIS bands 1, 2, and 5 and three angles (solar zenith, sensor zenith and the relative azimuth angle between the sun and the sensor). Two types MODIS data can be used as input, MODIS 1B data from the receiving station or MOD09 product downloaded from the NASA data center (either containing angular information which is used by the LAI estimation algorithm). The procedure is described below, separately for each case.

Scheme 1 (*MODIS 1B data as input*): The MODIS 1B data include 36 bands data and the geometric information on solar zenith, sensor zenith, solar azimuth, sensor azimuth, and geographical position. First, these reflectance data were atmospherically corrected by a dark object method (Kaufman et al., 1997). Although this approach is only suitable for vegetated regions, it is adequate for LAI retrieval. Next, all the input data were resampled to a new coordinate system. To minimize the influence of cloud and shadows, image compositing procedures are required to create 'representative' land surface reflectance data sets for periods when the surface conditions can be considered static. Various compositing approaches, such as maximum brightness temperature, minimum visible reflectance, maximum vegetation index or their combination, have been proposed to fulfill different objectives in order to minimize the clouds, shadow and aerosol contamination (Cihlar et al., 1994), among which the most common two methods are the selection data with the maximum NDVI (MNDVI) or selection of minimum blue band. Although it has been shown that the MNDVI can result in selection of off-nadir data (Cihlar et al., 1994) and cloud retention over certain land cover types, it is believed to minimize cloud cover, thus enhancing the vegetation signal. We used the MNDVI compositing method to produce 8-days clear land surface reflectance data sets.

Scheme 2 (*MODIS land surface reflectance product* (*MOD09*) *as input*): The MOD09 product is computed from the MODIS Level 1B land bands 1, 2, 3, 4, 5, 6, and 7 (centered at 648, 858, 470, 555, 1240, 1640, and 2130 nm, respectively; Vermote et al., 2002). The product is an estimate of the surface spectral reflectance for each band as it would have been measured at ground level if there were no atmospheric scattering or absorption. The correction scheme includes corrections for the effect of atmospheric gases, aerosols, and thin cirrus clouds. The input data for driving atmospheric correction are MODIS band 26 for cirrus, MOD05 for vapor, MOD04 for aerosol and MOD07 for ozone. If these data are unavailable in some regions, the accessory climatology may be used. Current land surface reflectance products do not correct the aerosol effect over bright regions because no aerosol data in these regions are contained in the MOD04 product. The single scene MOD09 data were composited over 8-day periods using the minimum blue channel method.

2.4. LAI data output

The output data include the LAI and effective LAI, ranging from 0 to 10. These values were scaled from 0 to 100 and saved as 8-bit integers. Sinusoidal projection was used for the product (the same as for the MODIS standard product, and Albers equal area projection, which is usually employed in other Chinese data, is optional). The LAI output resolution can be 250, 500 or 1000 m. The outputs were stored by tile in HDF or geotiff formats, each title covering 1200 km × 1200 km. The output files also include the quality status of the pixel from input land reflectance data, such as snow, cloud, shadow, clear and uncertainty.

2.5. Multi-temporal LAI interpolation

The retrieved LAI product is usually degraded by exterior noise, such as cloud screening, poor atmospheric condition, heavy aerosol or missing data. Such undesirable noise conceals the true vegetation condition and limits the LAI utility. Many methods have been developed to reduce that noise. The multi-day compositing method can remove most noise from atmosphere conditions. However, it is very difficult to get high quality LAI data in every pixel, especially in cloudy regions. In order to drive ecosystem models to get consistent results, input data in every pixel with a realistic season variation are required. In previous research, several time series interpolation methods were used to remove the noise pixel from multi-temporal data, such as BISE method (Viovy et al., 1992), Fourier-based fitting method (Roerink et al., 2000), and the locally adjusted cubic-spline capping method (Chen et al., 2006). In this paper, a wavelet transform method of Lv et al. (2006) was used to remove noise from the multi-temporal data. This method first removes the contaminated dates using the pixel quality status flag, and then fills these dates with high quality data from other dates in the same pixel through linear interpolation. The wavelet transform was applied to the interpolation time-series data. The high frequency data was smoothed using the method proposed by Pan et al. (1999). The smoothed wavelet coefficients were inversely transformed to obtain smoothed time-series data. The interpolation results are shown in Fig. 1. The cloud effect can be found in northeast and southwest China from Fig. 1(a). After interpolation, LAI increased in these regions. With the residual noise removed from LAI products, these interpolated LAI values can be used to drive ecosystem models directly.

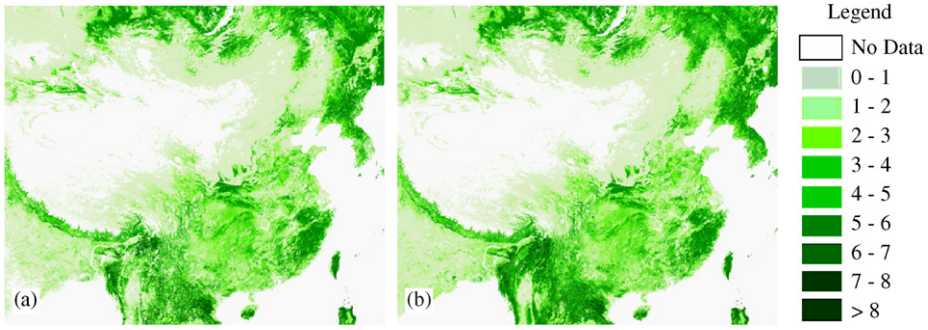

Fig. 1. Time-series interpolation to remove atmospherically contaminated pixels from multi-temporal data: (a) before interpolation and (b) after interpolation. Data day is 2003193, 16-days composite.

3. Results and validation

3.1. Uncertainty of LAI estimates

As stated above, the LAI retrieval results depend on land cover types, and thus the uncertainties of land cover classification could contribute to errors in LAI. To determine the uncertainties of LAI retrieval derived from land cover data sets in China, we evaluated the effects of five available land cover data sets on the LAI retrieval and compared them with the NASA MOD15 product. These data sets are: The Land Cover Map for Central Asia for the Year 2000 produced by Chiba University for GLC2000 database, European Commission Joint Research Centre (available: http://www.gvm.jrc.it/glc2000, 2003; thereafter referred to as Chiba); China Window data of GLC2000 produced by the Institute of Remote Sensing Applications, Chinese Academy of Sciences (available: http://www.gvm.jrc.it/glc2000, 2003; thereafter referred to as IRSA); The Chinese National Land cover data sets produced by the Institute of Geographical Sciences and Natural Resources Research, Chinese Academy of Sciences (Liu et al., 2003; thereafter referred to as NLCD); The MODIS enhanced land cover data sets produced by the University of Maryland (Zhan et al., 1999; thereafter referred to as UMD) and the global land cover data sets produced by the Boston University (Strahler et al., 1999; thereafter referred to as MOD12). The land cover classes of these data sets were aggregated to six vegetation classes and one non-vegetation class which correspond with the six functional types for LAI algorithms (Table 1). The input reflectances are 500 m MOD09 data, which cover all of China and date, is Julian day 209, 2003.

The LAI distributions in China derived with the different land cover data sets and MODIS LAI product are shown in Fig. 2, where we can find the IRSA-based LAI have the largest values in southern China. Other land cover data sets resulted in similar LAI distributions. The mean LAI values for all land surfaces with non-zero LAI values are shown in Table 2 for the various land cover data sets. The IRSA-based LAI had the highest mean value and the UMD-based LAI had the lowest one, with a relative difference of 27%. The pixel counts for each LAI increment are shown in Fig. 3. It is found that the pixel numbers for the five land cover data sets are similar for LAI below 4.0. Generally, the IRSA-based and the Chiba-based LAI products have more pixels with LAI above 5.0. The MOD12 LAI values were far higher than those based on the other land cover data sets.

Comparisons of the new LAI algorithm with the NASA MOD15 product were made using the same input land cover data sets. The new LAI product was produced using these MOD09 and MOD12 data sets as input to the new retrieval algorithm. Because MOD15 LAI also uses the MOD12 and MOD09 as input, the differences of two products are from the retrieval algorithm. A comparison of Fig. 2(a) and 2(e) shows that the MOD15 product has higher LAI values than the new LAI product. The mean value of MOD15 is 2.47, while the mean value for the new product is 1.95, resulting in a relative difference of 21%.

3.2. LAI validation

To validate the new LAI product, two sites with ground LAI measurements were selected. LAI measurements at these sites were made using an optical instrument TRAC (Tracing Radiation and Architecture of Canopies; Chen and Cihlar, 1995). TRAC measurements permit derivation of LAI as well as the clumping index. One experimental site is on the Qilian Mountain in Gansu Province at 38.7°N and 99.55°E with an elevation range from 2200 to 4800 m. The vegetation types are mountainous pasture and forest, which includes *Picea crassifolia,* and *Sabina przewalski*. The second experimental site is located on the north slope of the Changbaishan Natural Reserve in Jilin province ($41^0$42′N–$42^0$10′N, $127^0$38′–$128^0$10′E), and the elevation varies in the range from 720 to 2691 m. Vegetation is vertically stratified at this site and includes Korean pine and broadleaf mixed forest at elevations from 720 to 1100 m, spruce and fir forests from 1100 to 1800 m, *Betula ermanii* forest in the sub-alpine zone from 1800 to 2100 m, and alpine tundra above 2100 m. The Korean pine and broadleaf mixed forest are the dominant vegetation types.

On Qilian Mountain, 16 forest stands were chosen for the LAI measurement. The *Picea crassifolia* stands were distributed evenly in the research area. The ASTER image

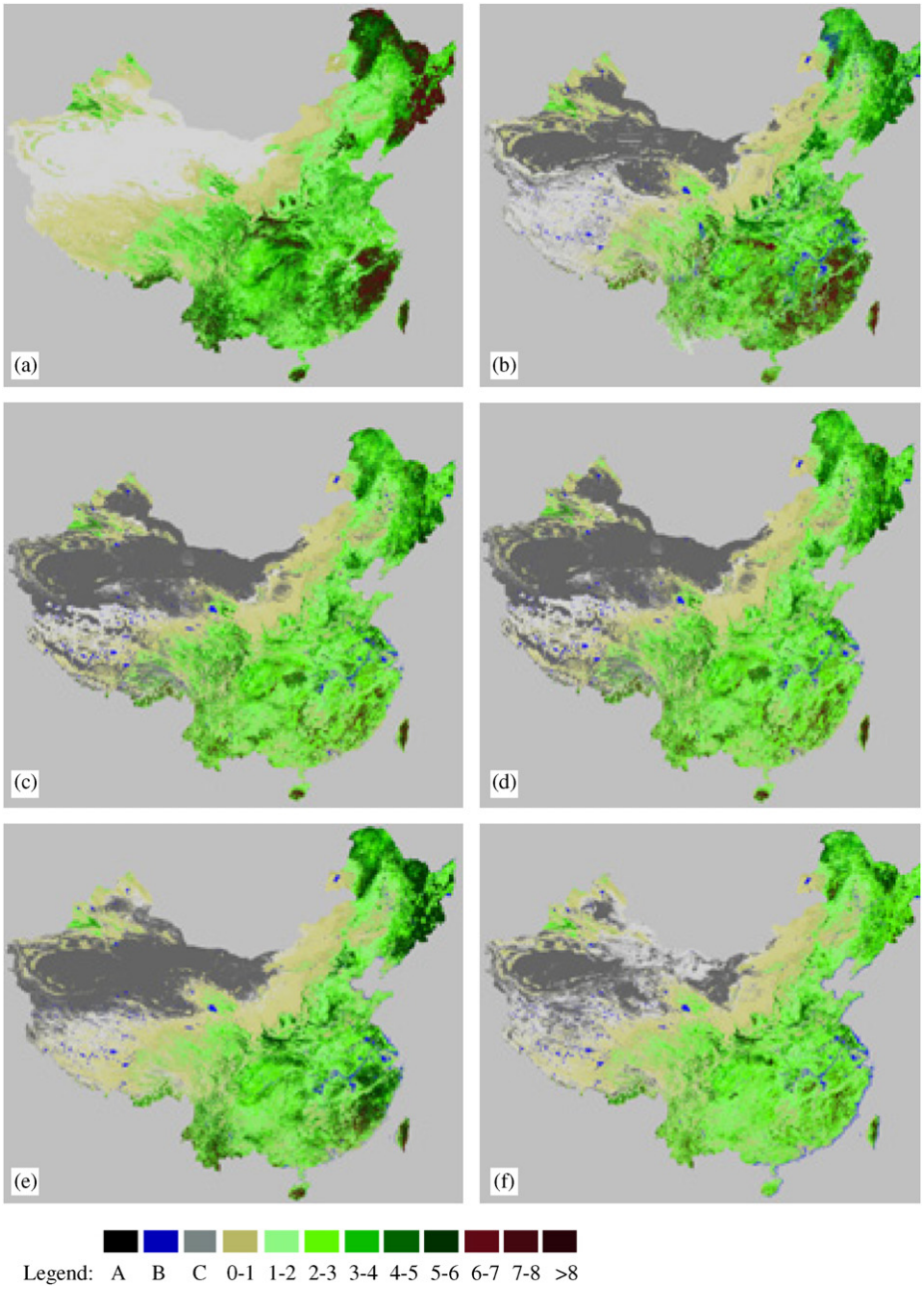

Fig. 2. The LAI distributions in China produced from using different land cover classifications (LCC): (a) MODIS MOD15 LAI product; (b) IRSA LCC-based LAI; (c) Chiba LCC-based LAI; (d) NLCD LCC-based LAI; (e) MODIS MOD12 LCC-based LAI (f) UMD LCC-based LAI. A is no data; B is water body and C is non-vegetation.

Table 2
Mean LAI values for land areas with non-zero LAI

IRSA	Chiba	NLCD	MOD12	UMD	MOD15
2.25	2.03	1.91	1.95	1.65	2.47

used for mapping LAI for this site was acquired on July 12, 2001. The image was corrected for atmospheric effects using 6S with the parameters acquired from the NASA MODIS products, and its geometry was corrected using ground control points. For the sample sites, the vegetation index NDVI was computed from the image, thus establishing the relationship between measured LAI and NDVI. The NDVI–LAI relationship for crop and grass was derived from other measurements in the same region, and an ASTER LAI map was produced using these relationships. The relationship for TRAC LAI and ASTER SR is $SR = 1.803 \times \ln(LAI) + 1.6275$, $R^2 = 0.6309$. To compare with the 1 km resolution LAI images from MODIS, this ASTER image at 20 m resolution was averaged to 1 km resolution by a resampling technique and then transformed the projection to Sinusoidal with same as MODIS LAI products.

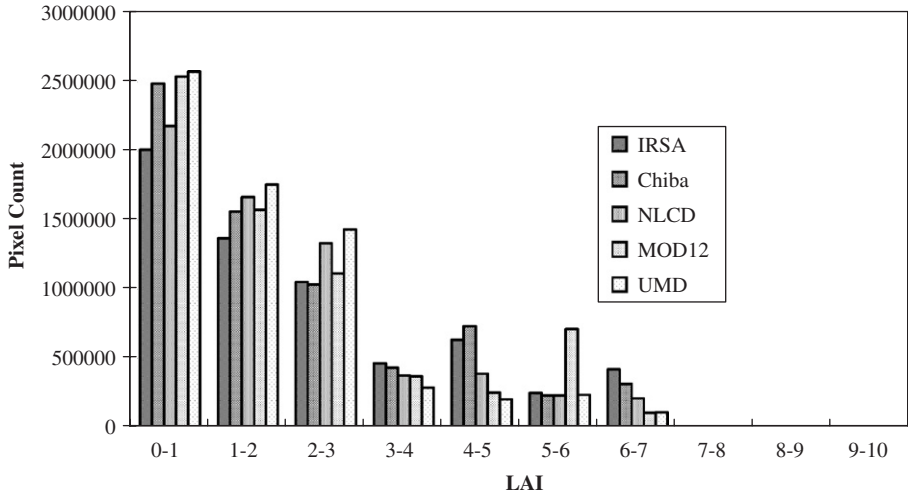

Fig. 3. Pixel counts in each LAI increment based on different land cover data sets.

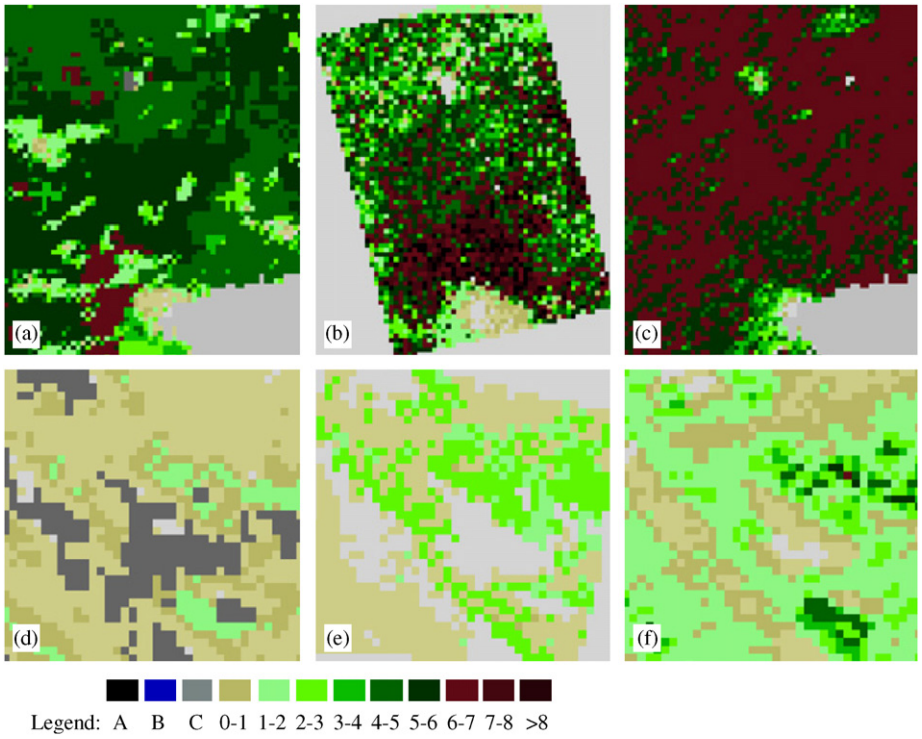

Fig. 4. Validation of LAI. (a) New product in Changbaishan; (b) Landsat TM LAI based on field measurements in Changbaishan; (c) NASA MODIS MOD15 product in Changbaishan; (d) New product in Qilian Mountain; (e) Landsat TM LAI based on field measurement in Qilian Mountain; (f) NASA MODIS MOD15 product in Qilian Mountain.

In the Changbaishan Natural Reserve, the LAI values were measured in 34 stands distributed evenly within each vertical zone. The LAI sampling area was 30 m × 30 m. In each stand, the canopy gap fraction and gap size distribution of four 30 m-long lines were measured using TRAC and the longitude and latitude were obtained by GPS. The field measurements were carried out on 5–9 September, 2002 and the Landsat TM data were acquired on August 25, 2002. The field LAI values were registered to the Landsat TM image and resampled to 1 km resolution for a comparison with MODIS products. The relationship for mapping LAI in Changbaishan was: $RSR = 14.57 - 14.57 \exp(-0.13LAI)$.

The validation results are shown in Fig. 4. In the Changbaishan region, the forests are dense as also indicated by the mean LAI values 5.08 for the new LAI product (Fig. 4(a)), 4.98 for the TM LAI map (Fig. 4(b)) and 5.97 for the NASA MOD15 product (Fig. 4(c)). The relative difference from Landsat TM LAI for the new LAI products and MODIS LAI products are 2% and 20%.

Both the magnitude and the spatial pattern of the new product matches the Landsat TM LAI map more closely than MOD15 (note the high LAI areas near the Tianchi Lake). The LAIs of MODIS products are generally larger than those of Landsat TM and their spatial distribution are more uniform than those derived from Landsat TM. MOD15 shows slightly lower LAI values near the Tianchi Lake than the other two products but rather high values in other forest regions.

In the Qilian Mountain region, forests are sparse with mean LAI values of 0.61 for the new LAI product (Fig. 4(d)), 0.99 for the ASTER LAI (Fig. 4(e)), and 1.64 for MOD15 (Fig. 4(f)). The new product is lower than field measurements by about 38%, while the MODIS product is larger by about 65%. Many similar spatial patterns of the LAI distribution can be identified among these products, but both the new product and MOD15 suffered from positive biases compared to the ASTER LAI image in terms of the magnitude and the area coverage, although these biases are much smaller in the new product than in MOD15.

4. Conclusions

This paper presents an integration of a BRDF-based LAI retrieval algorithm developed by Deng et al. (2006) into a MODIS data processing software MODISoft® to generate a new LAI product from MODIS 1B or MOD09 data. This LAI product has been validated against two forest sites in China. The results showed that the new LAI product compares more favorably with high-resolution LAI images produced with in situ measurements than the NASA MODIS LAI product MOD15. Uncertainties in LAI products resulting from different land cover data were also evaluated. The maximum mean LAI difference derived from different land cover maps reached 27% when averaged over the entire China's landmass. A time-series smoothing method was implemented to remove residual atmospheric contamination. The smoothed time series of LAI images can be used directly as input to ecosystem models without further processing.

Acknowledgments

This research was partially supported by CIDA project "Confronting global warming: enhancing China's capacity in carbon sequestration". Support also was provided through the grants from National 973 Program (No. 2002CB4125) and National Science Foundation of China (No.40471098).

References

Brown, L.J., Chen, J.M., Leblanc, S.G., 2000. Short wave infrared correction to the simple ratio: an image and model analysis. Remote Sensing of Environment 71, 16–25.

Chen, J.M., Black, T.A., 1992. Defining leaf area index for non-flat leaves. Plant Cell Environment 15, 421–429.

Chen, J.M., Cihlar, J., 1995. Plant canopy gap size analysis theory for improving optical measurements of leaf area index. Applied Optics 34, 6211–6222.

Chen, J.M., Cihlar, J., 1997. A hotspot function in a simple bidirectional reflectance model for satellite applications. Journal of Geophysical Research 102, 25,907–25,913.

Chen, J.M., Leblanc, S., 1997. A 4-scale bidirectional reflection model based on canopy architecture. IEEE Transactions on Geoscience and Remote Sensing 35, 1316–1337.

Chen, J.M., Pavlic, G., Brown, L., Cihlar, J., Leblanc, S.G., White, H.P., Hall, R.J., Peddle, D.R., King, D.J., Trofymow, J.A., Swift, E., Van der Sanden, J., Pellikka, P.K.E., 2002. Derivation and validation of Canada-wide coarse-resolution leaf area index maps using high-resolution satellite imagery and ground measurements. Remote Sensing of Environment 80, 165–184.

Chen, J.M., Deng, F., Chen, M., 2006. Locally adjusted cubic-spline capping for reconstructing seasonal trajectories of a satellite-derived surface parameter. IEEE Transactions on Geoscience and Remote Sensing 44, 2230–2238.

Cihlar, J., Manak, D., D'Iorio, M., 1994. Evaluation of compositing algorithms for AVHRR data over land. IEEE Transactions on Geoscience and Remote Sensing 32, 427–437.

Cohen, W.B., Maiersperger, T.K., Yang, Z., Gower, S.T., Turner, D.P., Ritts, W.D., Berterretche, M., Running, S.W., 2003. Comparisons of land cover and LAI estimates derived from ETM+ and MODIS for four sites in North America: a quality assessment of 2000/2001 provisional MODIS products. Remote Sensing of Environment 88, 233–255.

Deng, F., Chen, J.M., Plummer, S., Chen, M., 2006. Algorithm for global leaf area index retrieval using satellite imagery. IEEE Transactions on Geoscience and Remote Sensing 44, 2219–2229.

Fang, H., Liang, S., Kuusk, A., 2003. Retrieving leaf area index using a genetic algorithm with a canopy radiative transfer model. Remote Sensing of Environment 85, 257–270.

Kaufman, Y.J., Tanre, D., Remer, L., Vermote, E.F., Chu, A., Holben, B.N., 1997. Operational remote sensing of tropospheric aerosol over land from EOS moderate resolution imaging spectroradiometer. Journal of Geophysical Research 102, 17051–17067.

Knyazikhin, Y., Glassy, J., Privette, J.L., Tian, Y., Lotsch, A., Zhang, Y., Wang, Y., Morisette, J.T., Votava, P., Myneni, R.B., Nemani, R. R., Running, S.W., 1999. MODIS Leaf Area Index (LAI) and Fraction of Photosynthetically Active Radiation Absorbed by Vegetation (FPAR) Product (MOD15) Algorithm Theoretical Basis Document. Available: 〈http://eospso.gsfc.nasa.gov/atbd/modistables.html〉.

Liang, S., 2003. Quantitative Remote Sensing of Land Surfaces. Wiley, New York.

Liu, J.Y., Zhuang, D.F., Luo, D., Xiao, X., 2003. Land-cover classification of China: integrated analysis of AVHRR imagery and geophysical data. International Journal of Remote Sensing 24, 2485–2500.

Liu, R., Liu, J.Y., Liang, S., Chen, J. M., Zhuang, D., 2006. Mapping China using MODIS data: Method, software and data products. Journal of Remote Sensing, in press.

Lv, X., Liu, R., Liang, S., Liu, J., 2006. Removal of noise by wavelet method to generate the high-quality time series of terrestrial MODIS products. Photogrammetric Engineering and Remote Sensing, in press.

Myneni, R.B., Hoffman, S., Knyazikhin, Y., Privette, J.L., Glassy, J., Tian, Y., Wang, Y., Song, X., Zhang, Y., Smith, G.R., Lotsch, A., Friedl, M., Morisette, J.T., Votava, P., Nemani, R.R., Running, S.W., 2002. Global products of vegetation leaf area and fraction absorbed PAR from year one of MODIS data. Remote Sensing of Environment 83, 214–231.

Pan, Q., Zhang, L., Dai, G., Zhang, H., 1999. Two denoising methods by wavelet transform. IEEE Transactions on Signal Processing 47, 3401–3406.

Plummer, S., Olivier, A., Fierens, F., Chen, J.M., Dedieu, G., Muriel, S., Cramer, W., Philippe, C., Quegan, S., Schultz, S., Hoelzemann, J.,

2004. The GLOBCARBON Initiative: multi-sensor estimation of global biophysical products for global terrestrial carbon studies. In: ENVISAT-ERS Symposium Proceedings, Salzburg, Austria, 6–10 September 2004, European Space Agency, SP-572-ENVISAT.

Roerink, G.J., Menenti, M., Verhoef, W., 2000. Reconstructing cloudfree NDVI composites using Fourier analysis of time series. International Journal of Remote Sensing 21, 1911–1917.

Roujean, J.-L., Leroy, M., Deschamps, P.-Y., 1992. A bidirectional reflectance model of the earth's surface for the correction of remote sensing data. Journal of Geophysical Research 97 (D18), 20455–20468.

Sellers, P.J., Randall, D.A., Collatz, G.J., Berry, J.A., Field, C.B., Dazlich, D.A., Zhang, C., Collelo, G.D., Bounoua, L., 1996. A revised land surface parameterization (SiB2) for atmospheric GCMs, Part I: model formulation. Journal of Climate 9, 676–705.

Strahler, A.H., Moody, A., Lambin, E., 1999. MODIS Land Cover Product, Algorithm Theoretical Basis Document (ATBD), Version 5.0. Department of Geography, Boston University.

Turner, D.P., Cohen, W.B., Kennedy, R.E., Fassnacht, K.S., Briggs, J.M., 1999. Relationships between leaf area index and Landsat TM spectral vegetation indices across three temperate zone sites. Remote Sensing of Environment 70, 52–68.

Vermote, E.F., Saleous, N.Z., Justice, C.O., 2002. Atmospheric correction of MODIS data in the visible to middle infrared: first results. Remote Sensing of Environment 83, 97–111.

Viovy, N., Arino, O., Belward, A.S., 1992. The best index slope extraction (BISE): a method for reducing noise in NDVI time-series. International Journal of Remote Sensing 13, 1585–1590.

Wang, Y., Tian, Y., Zhang, Y., El-Saleous, N., Knyazikhin, Y., Vermote, E., Myneni, R.B., 2001. Investigation of product accuracy as a function of input and model uncertainities: case study with SeaWiFS and MODIS LAI/FPAR algorithm. Remote Sensing of Environment 78, 296–311.

Zhan, X., Hansen, M., DeFries, R., Townshend, J.R.G., Huang, C., Dimiceli, C., Sohlberg, R., 1999. MODIS Enhanced Land Cover and Land Cover Change Product, Algorithm Theoretical Basis Documents (ATBD) Version 2.0. EOS Project Office Document at Goddard Space Flight Center, Greenbelt, MD, 94p.